P1B.4 COMPARISONS OF LDAR NETWORK HEIGHT AND DENSITY DATA WITH WSR-88D ECHO TOP AND SCIT REFLECTIVITY DATA

Nicholas W. S. Demetriades*, Ronald L. Holle and Martin J. Murphy
Vaisala, Tucson Operations

1. INTRODUCTION

Three-dimensional radar reflectivity data and the algorithms used to help meteorologists interpret these data are extremely important in nowcasting. However, a number of inherent problems arise when tracking thunderstorm cells with 3-dimensional reflectivity. These problems include (1) identifying cells in a complex multi-cellular thunderstorm environment, (2) detecting thunderstorm cells at close range from the radar, (3) Storm Cell Identification and Tracking (SCIT) echo top altitude trends that exaggerate or misidentify thunderstorm growth and decay (Howard et al., 1997), and (4) volume scans that take 5 minutes to complete. Lightning Detection and Ranging (LDAR) provides another 3-dimensional thunderstorm dataset that has the potential to both complement and supplement WSR-88D reflectivities.

LDAR detects the very high frequency RF pulses (60-66 MHz) that are produced by both cloud and cloud-to-ground (CG) lightning flashes in three dimensions. The median location error for RF pulses detected within the interior of the Kennedy Space Center (KSC) LDAR network is 100 m. The expected flash detection efficiency of the KSC LDAR network is greater than 95 percent. Another important feature of LDAR is its ability to provide all three dimensions of these data simultaneously and in a continuous datastream. We have found that all of these features of LDAR allow us to identify thunderstorm cells and monitor important cell altitude trends very accurately. Lightning altitude trends have already been shown to successfully represent thunderstorm growth and decay in air mass storms (Lhermitte and Krehbiel 1979). A complete description of the KSC LDAR network used in this study can be found in Lennon and Maier (1991).

This paper will summarize important complementary features that LDAR can provide to radar reflectivity. For some cases of known radar deficiencies, it will be shown that LDAR data could serve as a substitute for radar data.

2. METHODOLOGY

Reflectivity data from the Melbourne, FL WSR-88D were used to make comparisons to the KSC LDAR network. The actual cell identification and echo top trends were obtained using output from version 3.2 of the SCIT algorithm (Johnson et al. 1998).

In order to identify thunderstorm cells, lightning density plots were created once every 5 minutes using ~1 km^2 grids. A linear scale was used for displaying the density values. The maximum density value of the linear scale for each plot depended on the lightning production of that storm. A time period of 5 minutes was used because this was the longest time that lightning could be displayed before storm propagation and new storm development began to cause lightning contamination from other cells, and it corresponds closely with the length of a radar volume scan.

The lightning top that was used for comparisons with the echo top was calculated using the following procedure. Lightning pulses were restricted to those that occurred within the convective core. This was accomplished by using only those lightning pulses within 3 km of the center point of the cell, which was defined as the center of the highest ~9 km^2 lightning density areas as shown on the 5-minute lightning density plots. The 95th percentile altitude of lightning pulses within the cell was then computed every 2 minutes from this dataset.

3. THUNDERSTORM CELL IDENTIFICATION

3.1 *25 July 1997*

Figure 1 shows a composite reflectivity image of a thunderstorm (cell 1) and adjacent thunderstorms that were identified by SCIT at 2323 UTC 25 July 1997. SCIT performed well by identifying cells 6, 1 and 17 which are visible with reflectivities above 57 dBZ (black).

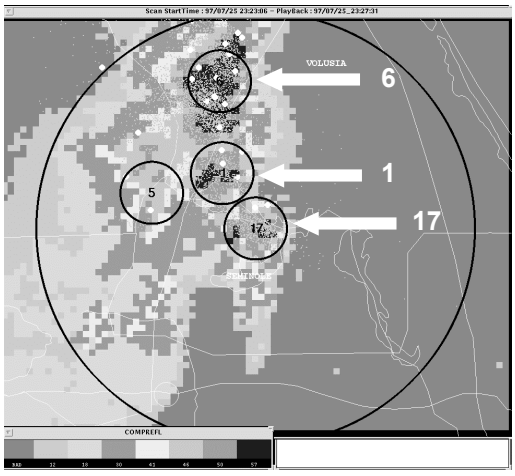

Figure 1. Melbourne, FL WSR-88D composite reflectivity image from 2323 UTC 25 July 1997. Cells are circled and labeled according to cell ID number. The small, gray dots are LDAR-detected RF pulses.

* *Corresponding author address:* Nicholas W. S. Demetriades, Vaisala, Tucson, AZ 85706-7155; email: nick.demetriades@vaisala.com

Figure 2 shows the KSC LDAR lightning pulse density plot from the closest 5-minute interval to the radar image in Figure 1. High density lightning cores made cells 6, 1 and 17 easily visible. These two figures demonstrate LDAR's ability to locate cells after they start producing lightning (i.e. become thunderstorms).

Figure 3 shows the difficulty of cell identification within a complex multi-cellular environment using reflectivity data and SCIT. Notice how SCIT misplaced cell 1 as the bottom portion of cell 6. It is not surprising that SCIT was confused because cell 1 is hard to make out visually given the reflectivity pattern. In this situation LDAR complemented radar because the lightning produced by cells 6, 1 and 17 identified three separate and distinct cells (Fig. 4). The highest level of lightning density values (most continuous gray shade) has more uniform coverage over the area of cell 1 than the highest level of reflectivity (black).

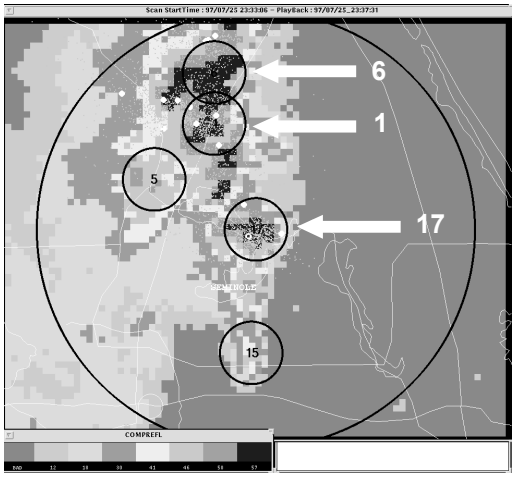

Figure 3. Same as Figure 1, except for 2333 UTC.

3.2 *6 July 1997*

Another complex multi-cellular thunderstorm environment developed on 6 July 1997. Figure 5 shows a large area of scattered high reflectivity (≥ 46 dBZ) with a well-defined cell that SCIT identified as cell 8. The LDAR density image from the closest 5-minute interval to this radar volume scan clearly identified this cell (Fig. 6). LDAR also detected another cell developing to the northeast of cell 8. SCIT did not identify this new cell yet, probably because it is hard to define a new cell within the reflectivity data at that location. During the next volume scan cell 8 decreases in reflectivity and the cell to its northeast increases in reflectivity (Fig. 7). This caused SCIT to misidentify cell 8 as the new cell that was developing to its northeast. The original cell 8 can be seen visually, however it is not easily identifiable. The LDAR density image from this time clearly shows the original cell 8 and could have prevented this misidentification (Fig. 8).

Figures 7 and 8 also demonstrate the complementary nature of radar and LDAR. In order for LDAR to identify a cell it must be producing lightning. Figure 8 shows that the new cell located to the northeast of cell 8 did not produce any lightning between 1830 and 1835 UTC. Therefore, radar alone would have identified this new cell that LDAR temporarily lost, and LDAR would have helped radar correctly identify the original cell 8. Lightning quickly redeveloped within the new cell between 1835 and 1840 UTC (not shown).

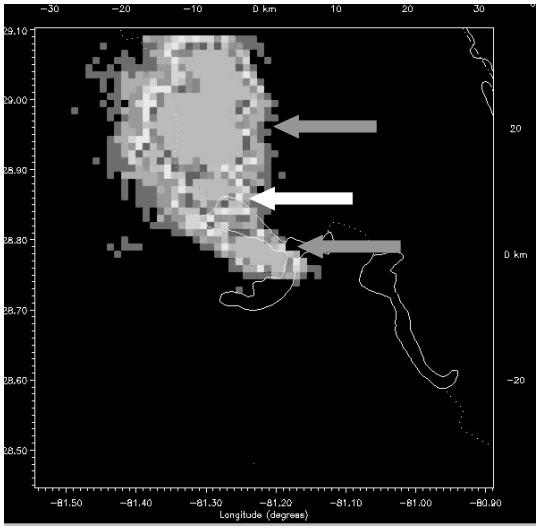

Figure 2. KSC LDAR density image created from lightning pulses detected between 2325 and 2330 UTC 25 July 1997. The white arrow points to cell 1 and the gray arrows point to cells 6 and 17.

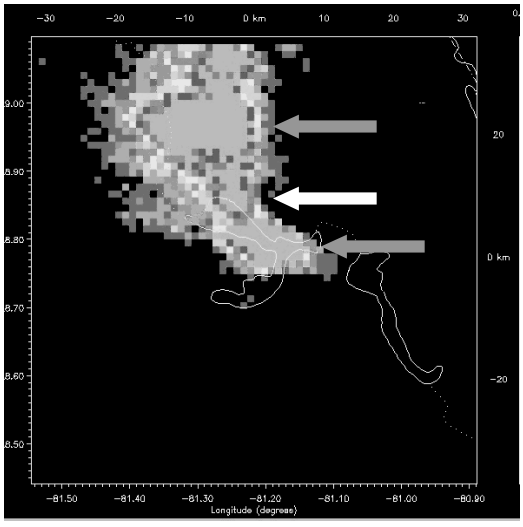

Figure 4. Same as Figure 2, except for KSC LDAR data detected between 2335 to 2340 UTC. The white arrow points to cell 1 and the gray arrows point to cells 6 and 17.

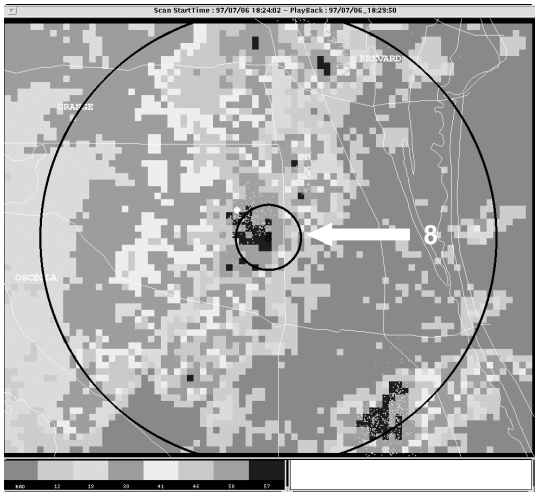

Figure 5. Same as Figure 1, except for 1824 UTC 6 July 1997.

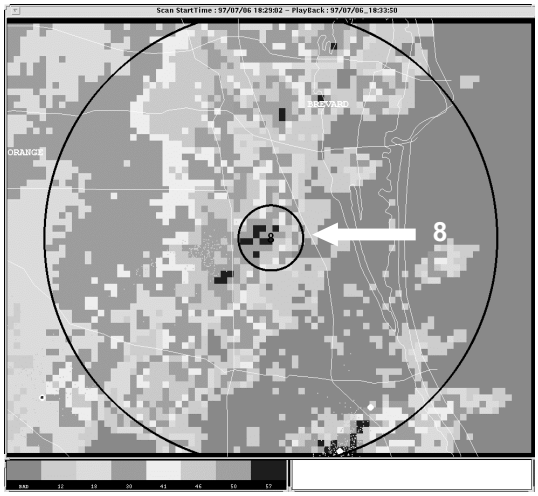

Figure 7. Same as Figure 5, except for 1829 UTC.

4. RADAR ECHO TOP AND LDAR LIGHTNING TOP COMPARISONS

4.1 *25 July 1997*

The echo top and lightning top data for this case came from the thunderstorm (cell 1) that was discussed earlier in Section 3.1. Figure 9 shows the echo tops and lightning tops from this case. This cell started at a distance of ~110 km to the northwest of the Melbourne WSR-88D and propagated toward the northeast. The echo top that SCIT calculated from this storm began at 12 km and then quickly started a rapid descent. Between 2317 and 2327 UTC the echo top fell from 12 to 4 km and then rose to 12.5 km at 2332 UTC. Part of this descent is probably real because the lightning top initially starts to descend around 2317 UTC. However, the continued descent to 4 km and rapid rise to 12.5 km are exaggerated representations of this storm's growth and decay. We do not know the exact cause of this drop and ascent, but it likely involves some combination of cell misidentification and storm motion through different tilts of the radar volume scan at long range. By 2321 UTC, the lightning top was already increasing again and radar reflectivities were growing within the cell (not shown). In fact, the lightning top remained at a fairly constant altitude (~14 km) while the echo top descended to 4 km and then rose again to 12.5 km. By 2337 UTC, the echo top did not even belong to the proper cell anymore because of SCIT's misidentification (see Section 3.1).

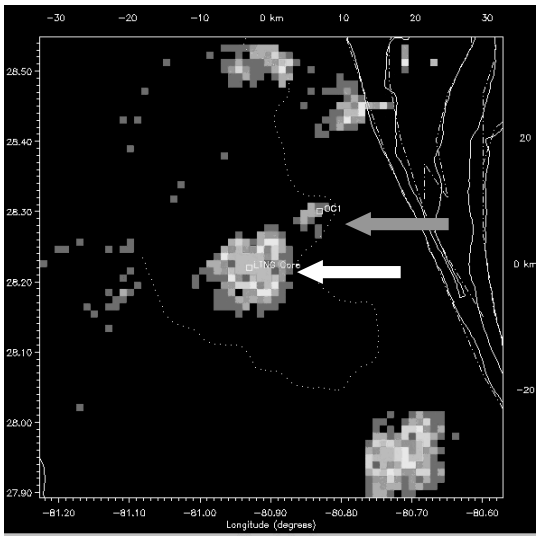

Figure 6. Same as Figure 2, except for KSC LDAR data detected between 1825 and 1830 UTC 6 July 1997. The white arrow points to SCIT cell 8 and the gray arrow points to a new cell that is developing to its northeast.

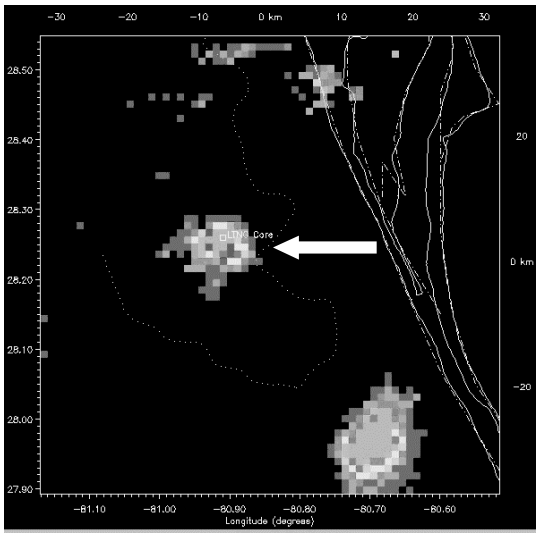

Figure 8. Same as Figure 6, except for KSC LDAR data detected between 1830 and 1835 UTC. The white arrow points to the original cell 8.

4.2 *9 July 1997*

Figure 10 shows the echo and lightning top analysis for a storm that occurred on 9 July 1997. At 2107 UTC, this cell was located ~50 km due north of the Melbourne WSR-88D. During the next hour, it propagated due south and moved into the WSR-88D cone of silence. This is clearly evident from the echo top analysis that shows a gradual descent from 12 km at 2107 to 3 km at 2152 UTC. The lightning top analysis initially shows a slight ascent and then levels off at ~14 km until 2134 UTC. The radar reflectivities also remained consistently high between 2107 and 2134 UTC (not shown). After 2134, the lightning tops gradually ascended until they reached 15.5 km at 2146 UTC. The radar reflectivities also increased during this time period. During the lightning top ascent, the storm began producing dime-sized hail at 2143 UTC.

5. SUMMARY

Comparisons of LDAR with WSR-88D reflectivity data show that LDAR can complement and, at times, supplement radar reflectivity data for thunderstorm cell identification and growth and decay trends. The case studies examined in this paper demonstrate LDAR's ability to identify and track thunderstorm cells more accurately in some complex multi-cellular thunderstorm environments. Two major reasons are (1) LDAR's higher spatial resolution relative to WSR-88D, and (2) maxima in lightning activity aloft appear to be closely associated with convective cores only. LDAR data also showed great temporal continuity that not only aids in identifying cells but also potentially tracking them.

Altitude analyses from a number of storms showed that lightning altitude trends can provide a large improvement over SCIT echo top trends for tracking thunderstorm growth and decay. Exaggerated SCIT altitude trends were caused by cell misidentification and echo tops from cells moving between different vertical tilts of the radar beam. Other echo top misrepresentations were due to storms approaching the radar and gradually being caught in the cone of silence.

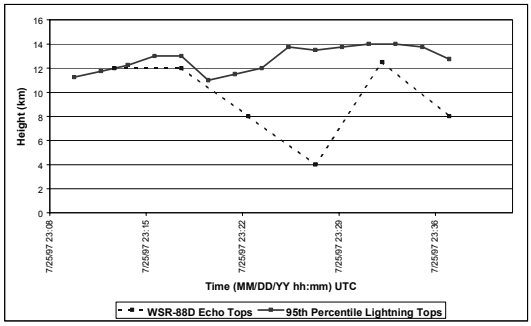

Figure 9. SCIT echo top trends obtained from the Melbourne, FL WSR-88D and lightning top trends calculated from the KSC LDAR network for the nonsevere thunderstorm (cell 1) that developed on 25 July 1997.

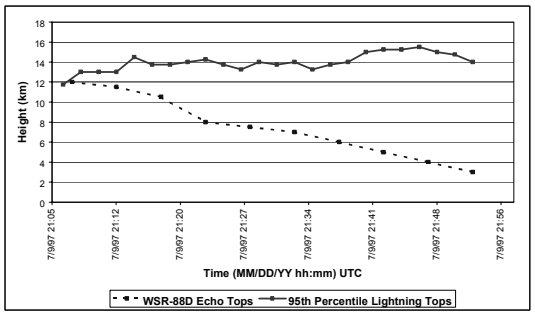

Figure 10. Same as Figure 9, except for the severe thunderstorm that produced dime-sized hail at 2143 UTC 9 July 1997.

Finally, the continuous data stream provided by LDAR allowed lightning altitude trends to be tracked on smaller time scales than the 5-minute updates of WSR-88D. This provided a higher level of detail for both thunderstorm growth and decay.

6. FUTURE WORK

We will continue to study thunderstorm cell identification and altitude trends using LDAR and radar reflectivity in different locations in order to address many of the issues raised by this study. Radar reflectivity data on constant altitude surfaces aloft will be used to further examine the possibility that LDAR defines individual cells better within certain thunderstorm environments because most of the lightning it detects is aloft. SCIT or a functionally similar cell-tracking algorithm will be run with LDAR density data to find if SCIT can identify individual cells better within complex multi-cellular thunderstorm environments using LDAR as a complement to radar reflectivity.

7. REFERENCES

Howard K.W., J.J. Gourley and R.A. Maddox, 1997: Uncertainties in WSR-88D measurements and their impacts on monitoring life cycles, *Wea. Forecasting*, **12**, 166-174.

Johnson, J.T., P.L. MacKeen, A. Witt, E.D. Mitchell, G.J. Stumpf, M.D. Eilts, and K.W. Thomas, 1998: The storm cell identification and tracking algorithm: An enhanced WSR-88D algorithm, *Wea. Forecasting*, **13**, 263-276.

Lennon, C., and L. Maier, 1991: Lightning mapping system, *Proceedings of the International Aerospace and Ground Conference on Lightning and Static Electricity*, Cocoa Beach, FL, NASA Conference Publication 3106, Vol. II, 89.1-89.10.

Lhermitte, R., and P.R. Krehbiel, 1979: Doppler radar and radio observations of thunderstorms, *IEEE Trans. Geosci. Electron.*, *GE-17*, 162-171.